SUPPLEMENTAL DATA for the paper:

Structure of Pleiotrophin- and Hepatocyte Growth Factor-binding Sulfated Hexasaccharide Determined by Biochemical and Computational Approaches

Fuchuan Li‡¶, Chilkunda D. Nandini¶, Tomohide Hattori#, Xingfeng Bao¶, Daisuke Murayama#, Toshikazu Nakamura†, Nobuhiro Fukushima#, and Kazuyuki Sugahara‡¶

‡*Faculty of Advanced Life Science, Hokkaido University Graduate School of Life Science, Sapporo 001-0021,* ¶*Department of Biochemistry, Kobe Pharmaceutical University, Kobe 658-8558,* #*Science & Technology Systems, Inc., Tokyo 113-0033, and* †*Kringle Pharma Joint Resarch Division, Center for Advanced Science and Innovation, Osaka University, Osaka 565-0871, Japan*

These supplemental materials comprise two parts:

(1) Supplementary tables S1, S2, and S3.

(2) Supplementary figures S1, S2, S3, S4, S5, and S6.

SUPPLEMENTARY TABLE S1

The dihedral angles (φ , ψ) of the geometry-optimized CS/DS oligosaccharides are listed (unit: degree). The $(2n+1)—(2n)$ glycosidic linkages correspond to the 1-3 linkages while the $(2n)—(2n-1)$ glycosidic linkages correspond to the 1-4 linkages (n : integer). Eight or six sugar residues of each octa- or hexasaccharide sequence have been numbered 1–8 from the reducing end.

glycosidic linkage	8-7		7-6		6-5		5-4		4-3		3-2		2-1	
	φ	ψ	φ	ψ	φ	ψ	φ	ψ	φ	ψ	φ	ψ	φ	ψ
ΔA-iB-iB	-	-	-	-	65.1	65.3	27.0	319.9	42.7	26.1	41.9	56.6	354.0	335.8
ΔC-A-A-A	37.5	34.6	358.9	1.9	39.5	7.5	24.1	24.8	11.2	327.7	2.8	0.5	24.6	30.7
ΔC-C-A-C	41.5	37.0	7.1	351.0	52.8	349.3	16.0	21.3	13.6	330.6	6.3	1.0	20.6	32.7
ΔE-D-A-D	71.3	48.4	31.8	313.5	51.4	24.5	51.8	42.3	7.9	329.7	29.5	317.2	40.4	13.7
ΔE-D-iA-D	40.6	40.4	17.6	341.6	47.8	351.0	26.8	49.3	342.3	337.7	19.4	2.0	24.3	8.8

SUPPLEMENTARY TABLE S2

Atomic point charges on ESP of the sulfate groups of the five isolated oligosaccharides

Sequence	S(2S)	O1(2S)	O2(2S)	O3(2S)	Sum(2S)	S(4S)	O1(4S)	O2(4S)	O3(4S)	Sum(4S)	S(6S)	O1(6S)	O2(6S)	O3(6S)	Sum(6S)
ΔAiBiB						**0.751**	**-0.514**	**-0.524**	**-0.523**	**-0.810**					
ΔA**iB**iB	**0.806**	**-0.522**	**-0.534**	**-0.578**	**-0.828**	**0.766**	**-0.526**	**-0.534**	**-0.536**	**-0.830**					
ΔAiB**iB**	**0.844**	**-0.525**	**-0.529**	**-0.555**	**-0.765**	**0.744**	**-0.516**	**-0.533**	**-0.538**	**-0.843**					
ΔEDAD						**0.735**	**-0.517**	**-0.528**	**-0.531**	**-0.841**	**0.775**	**-0.528**	**-0.532**	**-0.553**	**-0.838**
ΔE**D**AD	**0.810**	**-0.523**	**-0.529**	**-0.541**	**-0.783**						**0.708**	**-0.510**	**-0.511**	**-0.511**	**-0.824**
ΔED**A**D						**0.770**	**-0.513**	**-0.529**	**-0.543**	**-0.815**					
ΔEDA**D**	**0.753**	**-0.520**	**-0.524**	**-0.529**	**-0.820**						**0.703**	**-0.517**	**-0.520**	**-0.522**	**-0.856**
ΔEDiAD						**0.756**	**-0.518**	**-0.528**	**-0.533**	**-0.823**	**0.772**	**-0.537**	**-0.539**	**-0.546**	**-0.850**
ΔE**D**iAD	**0.911**	**-0.559**	**-0.579**	**-0.587**	**-0.814**						**0.783**	**-0.531**	**-0.533**	**-0.534**	**-0.815**
ΔED**iA**D						**0.763**	**-0.525**	**-0.544**	**-0.552**	**-0.858**					
ΔEDiA**D**	**0.789**	**-0.525**	**-0.535**	**-0.551**	**-0.822**						**0.739**	**-0.525**	**-0.534**	**-0.535**	**-0.855**
ΔCCAC											**0.724**	**-0.496**	**-0.501**	**-0.514**	**-0.787**
ΔC**C**AC											**0.768**	**-0.522**	**-0.522**	**-0.531**	**-0.807**
ΔCC**A**C						**0.754**	**-0.529**	**-0.530**	**-0.533**	**-0.838**					
ΔCCA**C**											**0.739**	**-0.506**	**-0.520**	**-0.529**	**-0.816**
ΔCAAA											**0.775**	**-0.516**	**-0.525**	**-0.555**	**-0.821**
ΔC**A**AA						**0.761**	**-0.519**	**-0.525**	**-0.53**	**-0.813**					
ΔCA**A**A						**0.735**	**-0.521**	**-0.526**	**-0.531**	**-0.843**					
ΔCAA**A**						**0.741**	**-0.509**	**-0.51**	**-0.516**	**-0.794**					

SUPPLEMENTARY TABLE S3

ESP atomic point charges of the carboxyl groups of the five isolated oligosaccharides[a]

	The first carboxyl group[b]				The second carboxyl group				The third carboxyl group				The fourth carboxyl group			
Sequence	**C**	**=O**	**-O-**	**Sum**	**C**	**=O**	**-O-**	**Sum**	**C**	**=O**	**-O-**	**Sum**	**C**	**=O**	**-O-**	**Sum**
ΔAiBiB	**0.692**	**-0.738**	**-0.768**	**-0.814**	**0.549**	**-0.693**	**-0.706**	**-0.850**	**0.628**	**-0.720**	**-0.756**	**-0.848**				
ΔEDAD	**0.654**	**-0.740**	**-0.761**	**-0.847**	**0.730**	**-0.751**	**-0.753**	**-0.774**	**0.733**	**-0.759**	**-0.773**	**-0.799**	**0.745**	**-0.743**	**-0.750**	**-0.748**
ΔEDiAD	**0.714**	**-0.757**	**-0.777**	**-0.820**	**0.731**	**-0.703**	**-0.770**	**-0.742**	**0.819**	**-0.745**	**-0.822**	**-0.748**	**0.816**	**-0.765**	**-0.776**	**-0.725**
ΔCCAC	**0.650**	**-0.736**	**-0.754**	**-0.840**	**0.677**	**-0.705**	**-0.746**	**-0.774**	**0.717**	**-0.761**	**-0.766**	**-0.810**	**0.708**	**-0.728**	**-0.758**	**-0.778**
ΔCAAA	**0.643**	**-0.736**	**-0.753**	**-0.846**	**0.761**	**-0.714**	**-0.768**	**-0.721**	**0.780**	**-0.765**	**-0.783**	**-0.768**	**0.689**	**-0.714**	**-0.740**	**-0.765**

[a]ESP atomic point charges were calculated according to the method reported in ref. S4.

[b]The three or four carboxyl groups are numbered from the non-reducing end to the reducing end.

SUPPLEMENTAL FIGURE LEGENDS

Supplementary Fig. S1. Comparison of the amino acid sequence of the major heparin-binding site of midkine with that of the corresponding sequence of pleiotrophin. Two amino acid sequences of midkine (entry 1MKC, Cys_{62}-Cys_{104}) at the position of the major heparin-binding site and pleiotrophin (PTN) (entry p63089, Cys_{99}-Cys_{141}) obtained by a pairwise sequence alignment are shown. Exact matching (orange) and similar (yellow) residues are demonstrated. Sequence identity and similarity are 54.5 and 77.3%, respectively, between 1MKC and p63089.

Supplementary Fig. S2. Isolation of the PTN-binding hexasaccharides from the size-defined hexsaccharide fraction prepared from SS-CS/DS-H. The size-defined hexasaccharide fraction prepared in the experiments shown in Fig. 3 was used to isolate a PTN-binding hexasaccharide under the same affinity choromatographic conditions as used in Fig. 4. These fractions, eluted with zero M (A), 0.15 M (B) and 0.5 M (C) NaCl in 10 mM Tris-HCl buffer (pH 7.4), were individually loaded on a Superdex^{TM} Peptide column, and eluted with 0.2 M NH_4HCO_3 while absorbance was monitored at 232 nm. The PTN-binding hexasaccharide fraction was collected as shown by a *bar* (B) and desalted by repeated lyophilization. For the elution positions of standard oligosaccharides indicated by *arrows*, see the legend to Fig. 3.

Supplementary Fig. S3. Fractionation of the PTN-binding hexasaccharides by anion-exchange HPLC. The PTN-binding hexasaccharide fraction, which was eluted with 0.15 M NaCl as shown in Supplementary Fig. S2-B, was resolved into constituents by anion-exchange HPLC on an amine-bound silica PA-03 column, using a linear gradient of NaH_2PO_4 as indicated by the *dashed line* (For details see "Experimental Procedures"). The major fraction M was desalted by gel-filtration on a Superdex^{TM} Peptide column using ammonium acetate and subjected to structural analysis. The broad peak marked by an asterisk and eluted after the peak M is often observed upon high sensitivity detection in a control chromatography without a sample, and contained no oligosaccharide at all as examined after desalting, suggesting that it is derived from the column.

Supplementary Fig. S4. Matrix-assisted laser desorption ionization time-of-flight mass spectrum of the compound M—An aliquot (10 pmol) of fraction M was mixed with a basic peptide $(Arg\text{-}Gly)_{15}$ (ref. S1) followed by a small volume of an aqueous solution (10 mg/ml) of a matrix, 2,5-dihydroxybenzoic acid (ref. S2). The mixture was placed on the sample plate, dried under an air stream, and analyzed. The matrix-assisted laser desorption ionization time-of-flight mass spectrum of the protonated complex of fraction M with $(Arg\text{-}Gly)_{15}$ was recorded in a positive ion mode in a Voyager DE-RP/Pro (PerSeptive Biosystems, Framingham, MA) (ref. S3). The observed mass of the minimal PTN-binding SS-CS/DS hexasaccharide shown in *brackets* was calculated by subtracting the value for the protonated peptide (3213.75 Da) from that for the protonated 1:1 complex (4749.49 Da).

Supplementary Fig. S5. Snapshots of the calculated ESP distribution of the five isolated oligosaccharides. The distribution of ESP was calculated for each isolated oligosaccharide, and electronegative (yellow) and electropositive (blue) zones are shown. *A*, ΔA-iB-iB; *B*, ΔE-D-A-D; *C*, ΔE-D-iA-D; *D*, ΔC-C-A-C; *E*, ΔC-A-A-A. The putative PTN-binding octasaccharides, ΔE-D-A-D and ΔE-D-iA-D, have spreading electronegative zones at iso-values of -0.5 ~ -0.7, and even ΔA-iB-iB hexasaccharide had a small yet detectable electronegative zone at -0.7 as shown in Figs. S5-1*A*, S5-2*B*, and S5-3*C*, respectively. In contrast, the non-binding octasaccharides, ΔC-C-A-C and ΔC-A-A-A, had no electronegative zones at -0.7 (Figs. S5-1~S5-3). The spread of the electronegative zones for the PTN-binding oligosaccharides was larger than that for the non-binding oligosaccharides at the same

iso-values. The iso-values are 0.5, 0.6, and 0.7 eV for the iso-surface of the electropositive zones and -0.5, -0.6, and -0.7 eV for that of the electronegative zones. These snapshots at the isovalues of ±0.5, ±0.6, and ±0.7 have been turned by 90 degrees around the axis from the non-reducing to the reducing end as shown in Figs. S5-1 ~ S5-3.

Supplementary Fig. S6. Predicted 3D structure of PTN. 3D structure of PTN was predicted by the homology modeling and the energy minimization, and constructed as detailed in "Experimental Procedures." The left and right figures display the front view of a stick and a space-filling model, respectively, to understand the frame and the cavity of the PTN molecule. The scales show the height and width of the PTN molecule. Red residues are corresponding to the basic cluster of midkine for heparin-binding and predicted based on the alignment with the midkine sequence, and are labeled with one-letter codes (right figure).

References

S1. Juhasz, P., and Biemann, K. (1995) *Carbohydr. Res.* **270,** 131-147
S2. Rhomberg, J., and Biemann, K. (1997) in *A Laboratory Guide to Glycoconjugate Analysis:* (Jackson, P., and Gallagher, J. T., eds) pp. 77-89, Birkhuser Verlag, Basel, Switzerland
S3. Yamada, S., Okada, Y., Ueno, M., Iwata, S., Deepa, S. S., Nishimura, S., Fujita, M., Van Die, I., Hirabayashi, Y., and Sugahara, K. (2002) *J. Biol. Chem.* **277,** 31877-31886
S4. Lee, M., Salsbury, F., and Brooks, C. (2002) *J. Chem. Phys*. **116,** 10606-10614

Supplementary Fig. S1

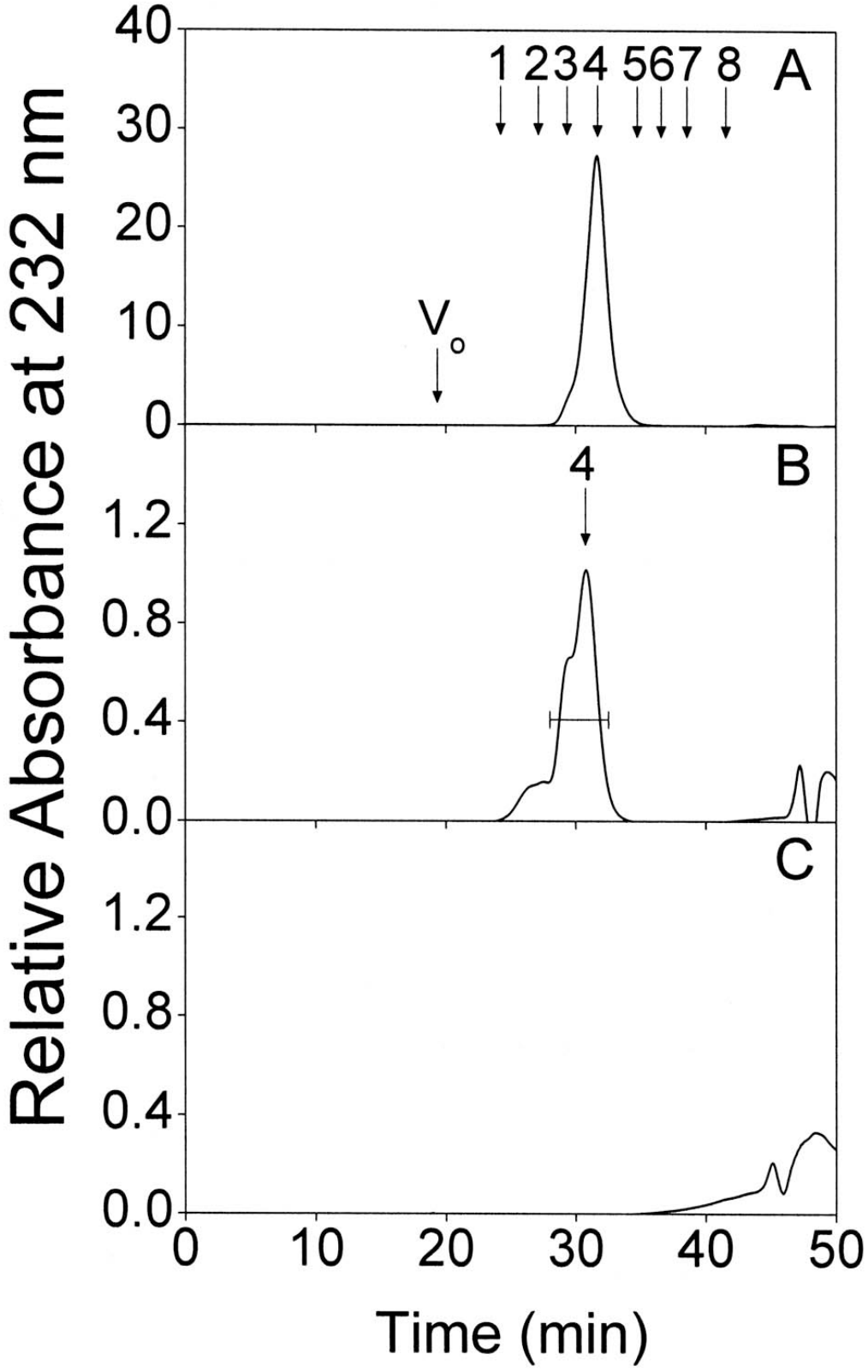

Supplementary Fig. S2

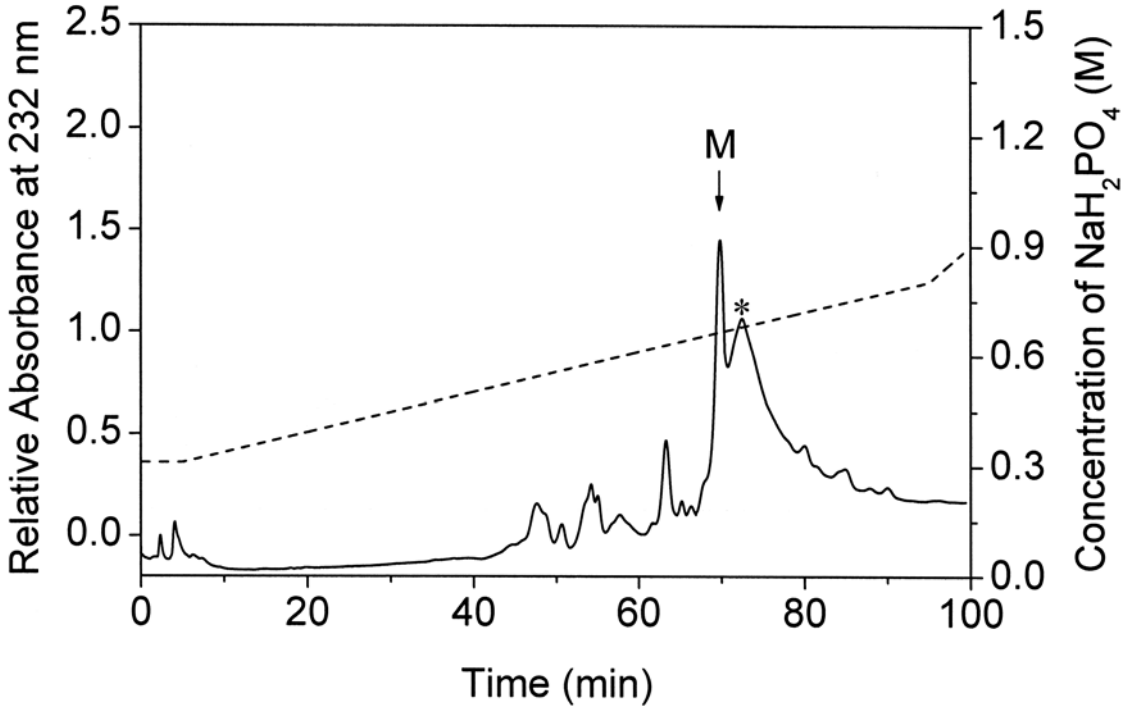

Supplementary Fig. S3

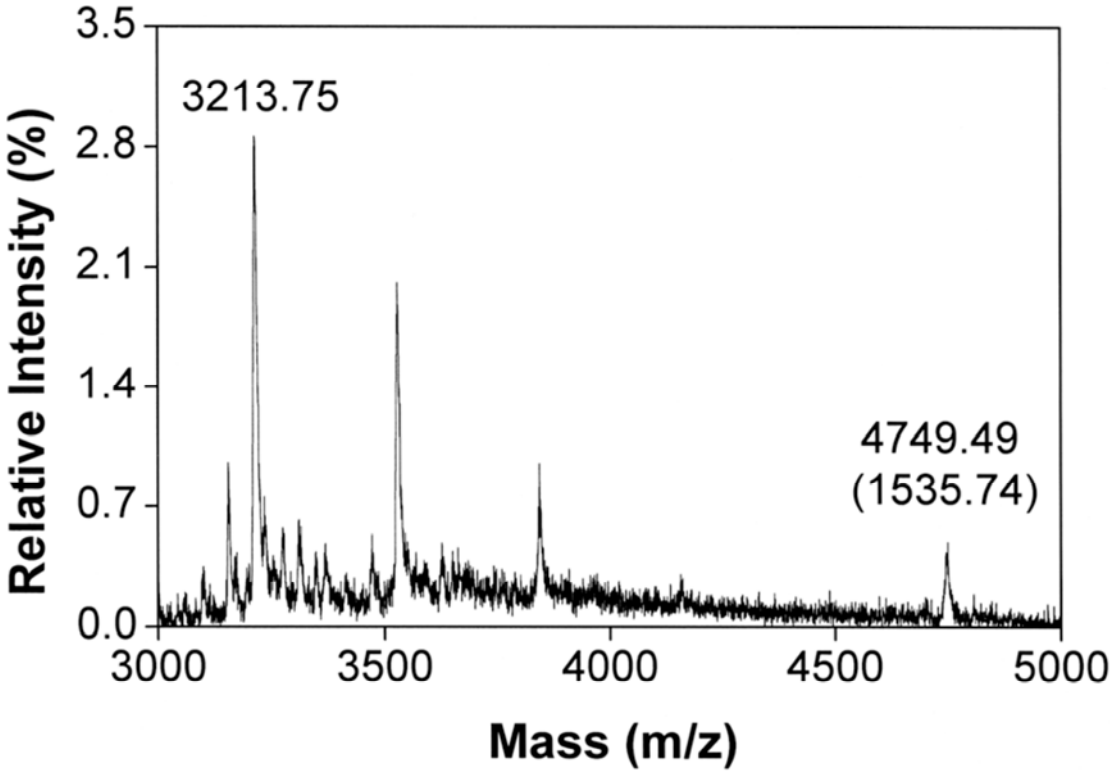

Supplementary Fig. S4

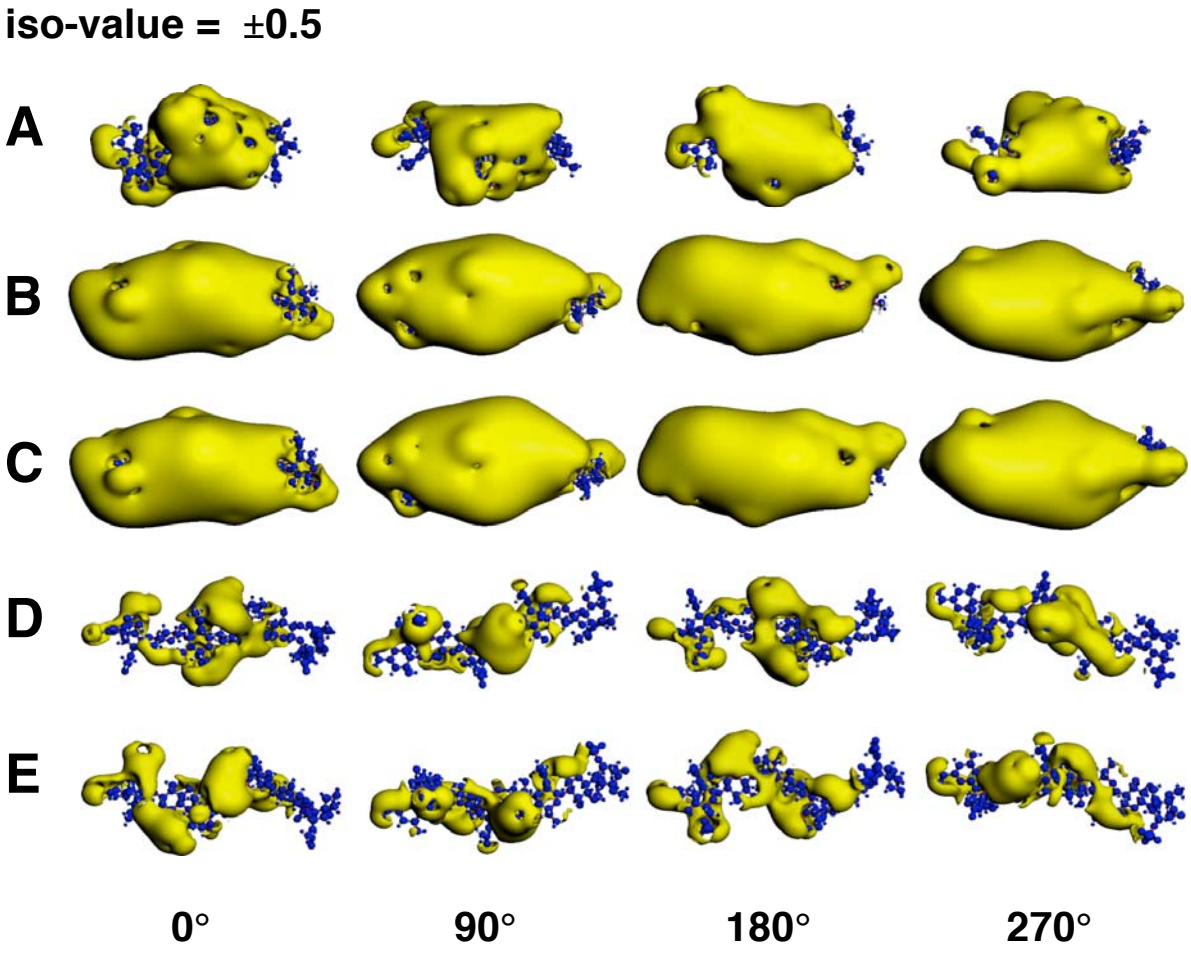

Supplementary Fig. S5-1

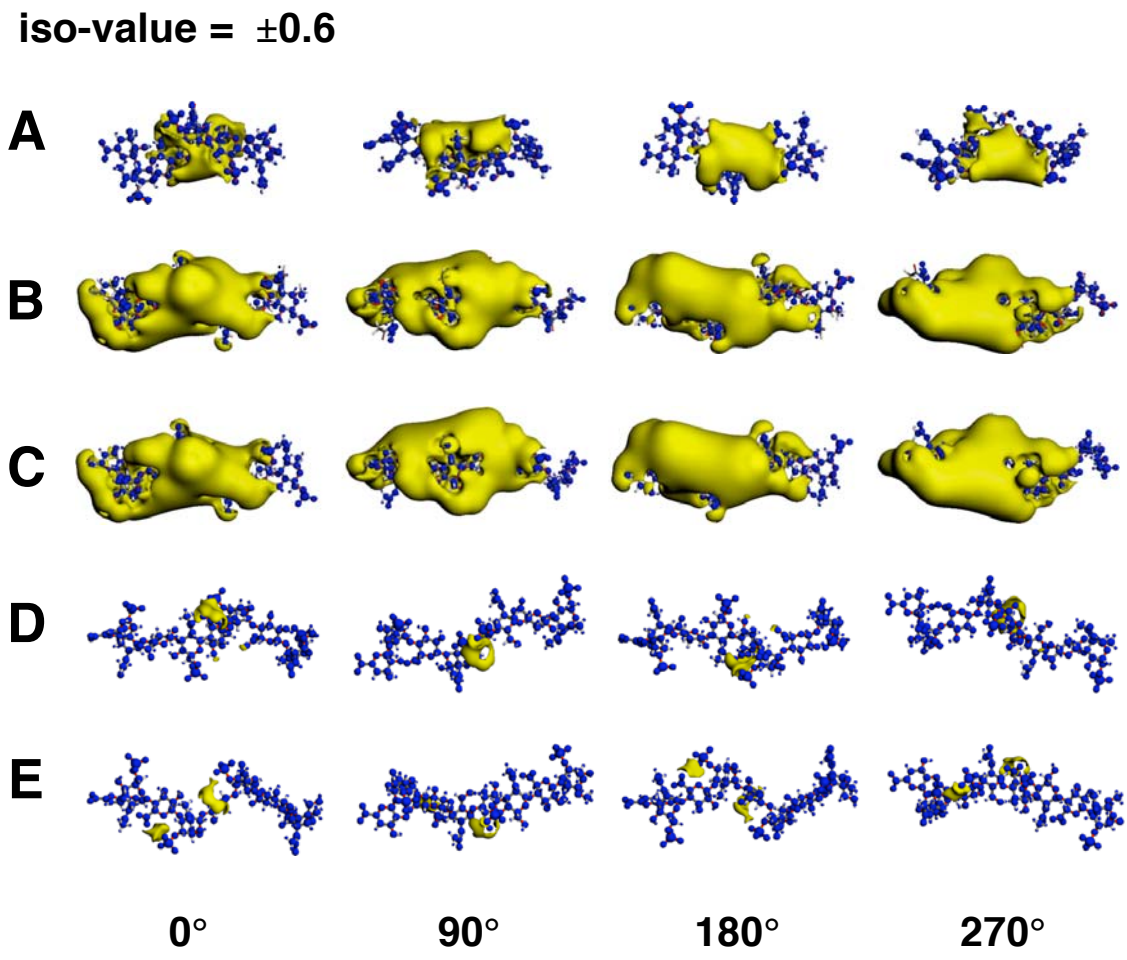

Supplementary Fig. S5-2

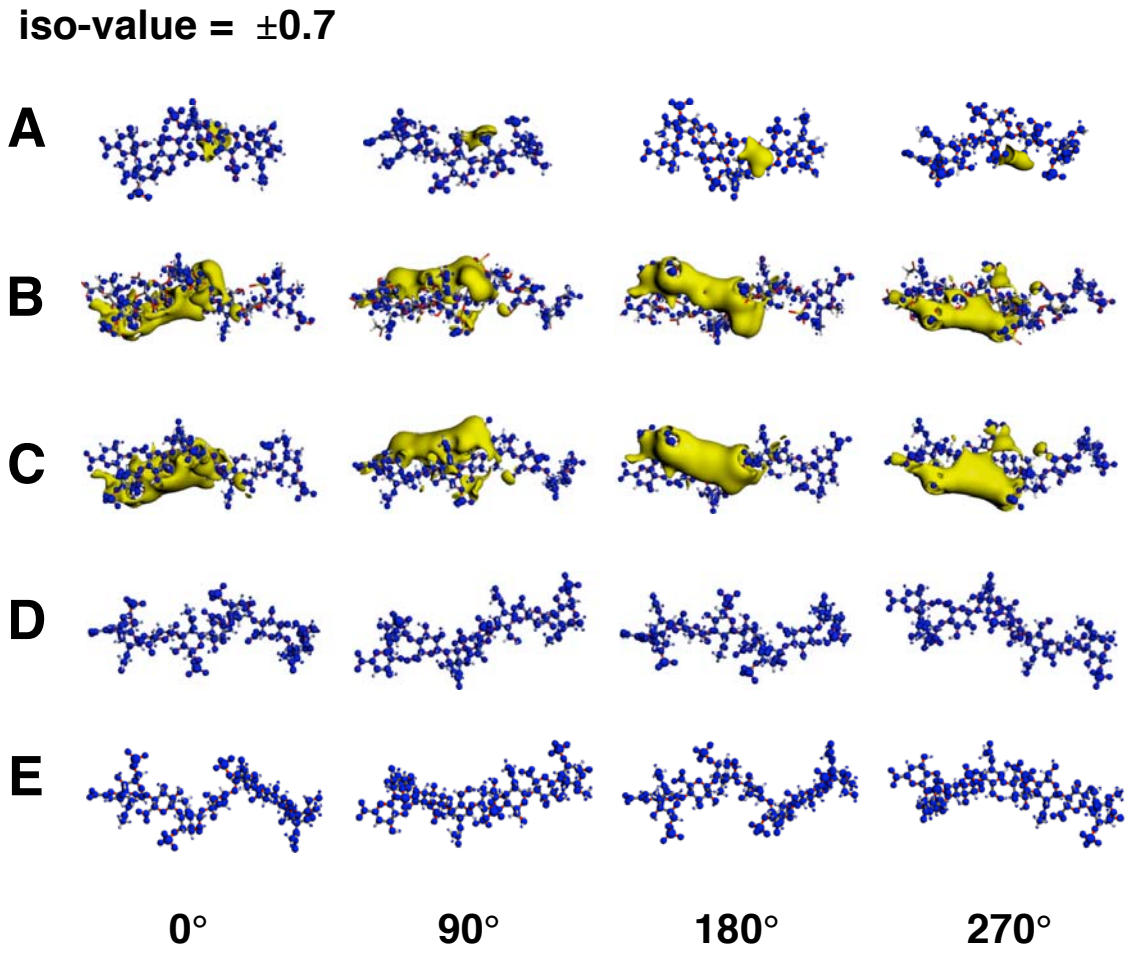

Supplementary Fig. S5-3

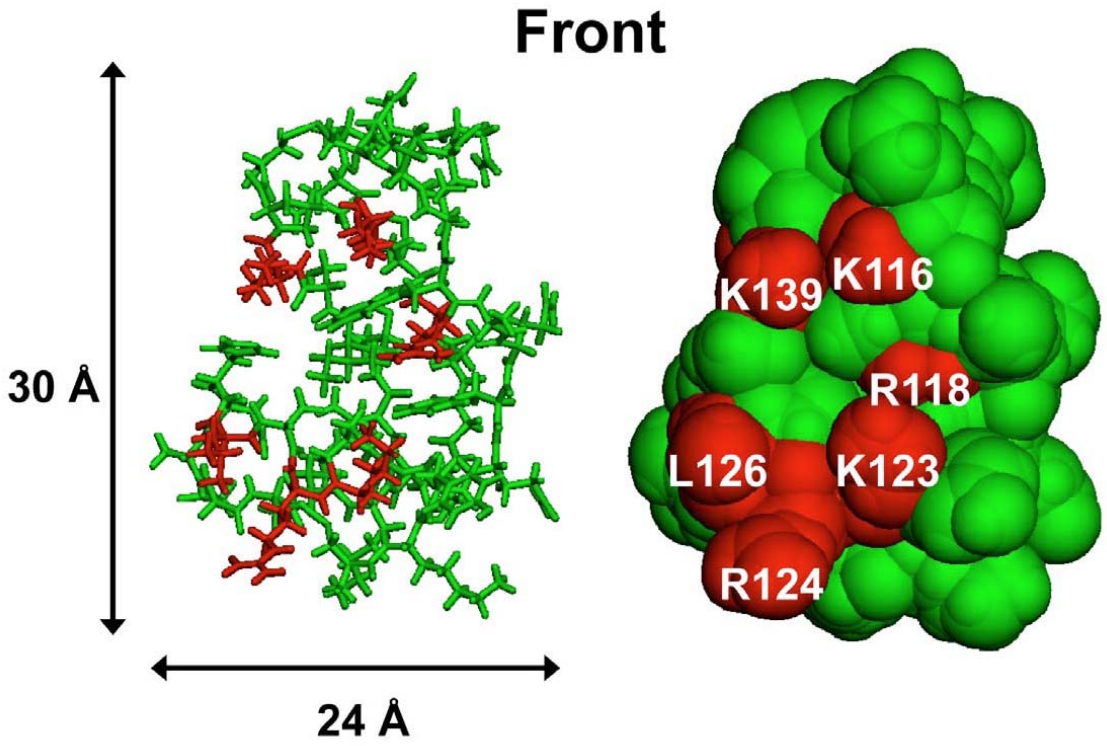

Supplementary Fig. S6